Journal of Building Engineering 49 (2022) 104078

Contents lists available at ScienceDirect

Journal of Building Engineering

journal homepage: www.elsevier.com/locate/jobe

Timber-concrete composite structural flooring system

J. Estévez-Cimadevila *, E. Martín-Gutiérrez, F. Suárez-Riestra, D. Otero-Chans, J. A. Vázquez-Rodríguez

Department of Architectural, Civil and Aeronautical Buildings and Structures, Universidade da Coruña, Spain

ARTICLE INFO

Keywords:
Timber-concrete composite
Timber flooring systems
Mixed beams
Shear connector

ABSTRACT

An integrated solution is presented for the execution of building structures using timber-concrete composite (TCC) sections that make efficient use of the mechanical properties of both materials. The system integrates flooring and shaped prefabricated beams composed of a lower flange of glued laminated timber (GLT) glued to one or more plywood or laminated veneer lumber (LVL) ribs and linked to an upper concrete slab poured in situ. The parts may be prefabricated in T shape (only one rib), in π shape (two ribs), or with multiple ribs to create wider pieces, thereby reducing installation operations.

The basis of the system is the timber-concrete shear connection in the form of holes through the ribs, which are filled by the in situ-poured concrete. The connection is complemented with the arrangement of reinforcement bars through the holes.

Three test campaigns were undertaken. Shear tests of the timber-concrete connection in 12 test pieces. Shear test along the wood-wood glue line (72 planes tested) and wood -plywood (24 planes tested). Delamination test of the glued planes (24 wood-wood planes and 8 wood-plywood planes). The results indicate a high strength joint, with ductile failure and high composite effect. Likewise, the shear test results along the glue line and the delamination tests show section integrity under demanding hygrothermal conditions.

Preliminary sizing curves were developed considering the Gamma Method to evaluate the performance of the system. The results show the possibilities of the system, as pouring the upper slab concrete in situ makes it possible to create continuous semi-rigid joints between the elements. This gives rise to slender flooring structures, light and with high stiffness plane against horizontal forces.

1. Introduction

There is no doubt that the construction sector is one of the main causes of the current climate emergency. According to studies [1], the construction and operation of buildings accounted for 38% of global final energy consumption and 38% of energy related CO2 emissions in 2015. By 2020, there have been improvements with around a fallen around 2% in demand and 10% in emissions. These reductions have been attributed party to the effect of the pandemic but mainly to actions that countries included to address building related emissions. In recent years, this situation has led to increasing interest in alternative building solutions which harm the ecosystem less and are more efficient. Within the structural context of multi-storey buildings, this search for greater ecological efficiency necessarily involves a reduction in the use of the most common structural materials (steel and concrete), mixing them with

* Corresponding author.
E-mail address: javier@udc.es (J. Estévez-Cimadevila).

https://doi.org/10.1016/j.jobe.2022.104078
Received 15 November 2021; Received in revised form 10 January 2022; Accepted 17 January 2022
Available online 22 January 2022

timber, a material that provides effective combination of good mechanical properties with well-known sustainability advantages [2,3]. This gradual introduction of wood into the field of multi-storey buildings has led to the development of many engineered wood products. Studies have also highlighted the importance of structural connectors and mechanical fasteners when evaluating environmental impacts in life cycle assessment (LCA) studies [4]. Hybrid structures and reduced connections seem like a solution worth exploring for mid- and high-rise building design. On the other hand, overall analysis of wooden structure sustainability in comparison with more usual materials reveals that massive usage may cause deforestation or forest degradation. This is because of the tendency towards monoculture of the most suitable species for use in the building sector, and these factors must be taken into account [3,5].

One of the main problems which arise due to the use of timber in multi-storey buildings is associated with the difficulty of creating rigid or semi-rigid joints. This often leads to the use of simply supported pieces, a solution that is inefficient in terms of strength and stiffness. Because of this, projecting timber-only long span buildings gives rise to structural solutions that consume large amounts of material [3]. The use of timber-concrete composite (TCC) systems can be a means of optimising structural solutions. The synergy between the properties of both materials makes it possible to achieve more efficient solutions in structural terms than only-timber structures. Hybrid structures also offer a substantial improvement in ecological efficiency in comparison with concrete-only structural systems. In any case, the advantages of TCC systems are known, and many references address these benefits [6–8].

The behaviour of TCC systems is based on the efficiency of the timber-concrete shear connection. An ideal joint aims to combine high strength against shear forces with low slippage of the connection, so that the composite effect makes it possible to take maximum advantage of the section in terms of stiffness, together with ductile behaviour. The technical literature describes the development of several timber-concrete connection systems, and these can be classified into three groups. The first group involves the use of steel fasteners such as nails or screws in different arrangements [9–19], or superficial systems such as steel plates inserted into the wood [20,21]. In general, although connections of this type vary in how much they tend to slip depending on their type and arrangement, their slippage reduces the composite efficacy of the solution. The second group of connectors includes glued solutions, such as bars [18,22,23] and plates [19–28]. Connections of this type slip less, improving their composite effect. Nevertheless, their drawback is that the use of structural adhesives is not very positive in terms of sustainability. Moreover, glued solutions in general are more demanding in terms of labour and monitoring of execution, given the time the adhesives used take to cure. Finally, the third group of connectors is based on the use of grooves or slots in the wood that permit the mechanical transmission of forces between the concrete and the timber.

These connections are very rigid thanks to the reduced slippage of the joint [29]. Nevertheless, they tend to undergo brittle failure, so that they are often combined with additional steel fasteners, which provide a ductile failure while maintaining a high stiffness in service [22,30–33].

This paper describes a TCC system based on a new connection between these materials using perforated boards. The system is complete and includes all the elements which form the structural flooring system: the flooring, beams and columns. Its high performance in terms of stiffness as well as strength permit long span designs using a reduced amount of materials, which in turn reduces its environmental impact.

2. Description of the system

The proposed system for the execution of building structures uses TCC sections that allows an efficient use of the mechanical qualities of both materials. The system is protected by the Spanish Office of Patents and Brands under reference ES1242743. It is composed of prefabricated wooden pieces with a modularity, simplicity and lightness that makes them easy to assemble on site, simplifying the execution process by eliminating the auxiliary elements used in connections. These prefabricated pieces are

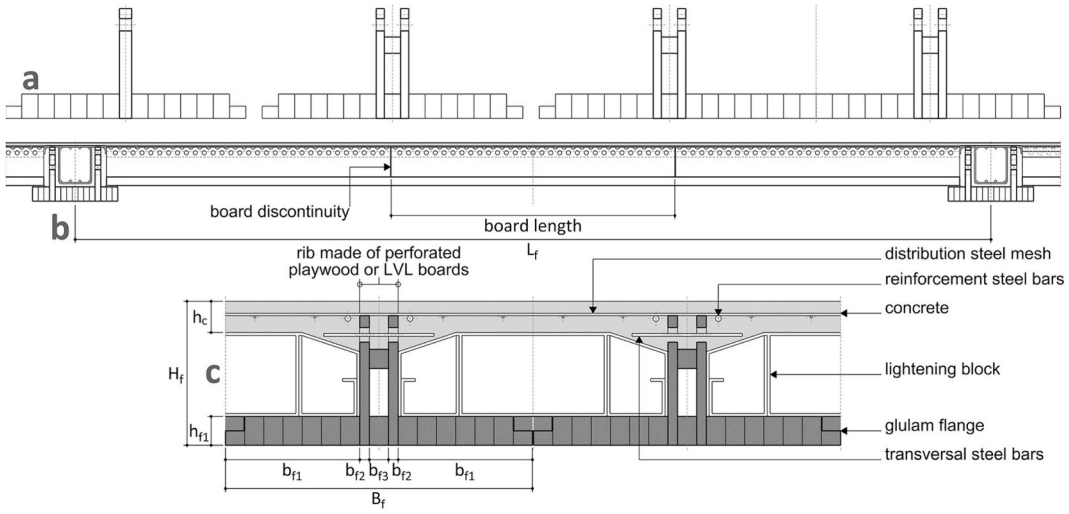

Fig. 1. a-Transversal cross-section of the different configurations of the prefabricated flooring part. b-Front view of the prefabricated flooring part. c-Elements within the flooring.

complemented by concrete pouring after the installation of steel bars reinforcement, which are necessary in the zones where floors are supported and on the beams and supports in structural frames. The basis of the system is the design of the new timber-concrete connection, characterised by the use of perforated plywood boards through which the concrete poured in situ forms a mechanical connection that has been proven to possess high stiffness, strength and ductility.

The system is composed of the following elements:

2.1. Floors

The floor is composed of a prefabricated T-shaped piece formed of a lower GLT flange glued to a rib made of plywood or LVL boards (Fig. 1-a). This rib may be simple, with a single board, or multiple with two or more boards, separated or not from each other. The upper part of these boards are transversally perforated throughout their entire length, allowing effective contact with the poured concrete. The piece may be prefabricated as a simple inverted T, or it may have multiple ribs to form wider cross-sections, thereby reducing the assembly work. The longitudinal joint between panels is made with a surface spline or cover strip timber piece which requires a milled-in joint in the edges of the glulam flange. This solution allows swelling and shrinkage of the glulam flange due to hygrothermal changes while ensuring the integrity of both fire resistance and acoustic insulation. The lower flange is continuous throughout its whole length; the rib may also be continuous, if LVL is used, or it may have discontinuities, if plywood is used, with the aim of fitting commercial dimensions and thereby making better use of the material (Fig. 1-b). The presence of two discontinuities in the board is not a drawback; on the contrary, the reduction in stiffness of the section at these points makes it possible to easily apply a precamber to compensate for deflections due to self-weight and shortening caused by concrete shrinkage. Fig. 1-c shows a cross-section of the floor with the prefabricated timber parts and the other components.

Light hollow blocks are arranged over prefabricated timber cross-sections (prototype in Fig. 2-a) acting as temporary formwork. Many commercially available models may be used such as EPS or solutions in recycled materials, or specifically designed models in cardboard, as shown in Fig. 2-b. Fig. 2-c shows the test performed to check the integrity and suitable functioning of the cardboard blocks during the concrete pouring. The set is complemented by the positioning of distribution steel mesh on the upper slab of the concrete to control shrinkage, reinforcement steel bars to prevent negative bending in the zones of continuous support of the floor, and transversal steel bars which pass through the holes in the board to improve the ductility of the connection. Finally, the whole floor is covered with a 50 mm thick concrete layer over the light blocks (Fig. 1-c).

2.2. Beams

The beams are formed in the same way as the flooring parts. They are composed of a prefabricated timber piece in the shape of an inverted π, formed by two ribs and a lower GLT flange which are laminated as a whole (Fig. 3-a). The GLT flange protrudes laterally from the ribs to serve as a support for the flooring parts, and its ends are machined to permit its connection to the supports. As is the case with the flooring, the plywood or LVL boards have holes throughout their length to transfer the shear forces between both materials. The set is completed by section reinforcing bars that are held in the space between both boards. This makes it possible to create a semi-rigid connection with the columns to which it is joined.

2.3. Columns

Although the horizontal structure of floors and beams may be supported on reinforced concrete or steel columns or walls, the system also includes a solution with TCC supports. In this case, rather than being used for its strength, the mixed section is used to facilitate and speed up the construction process. The supports are composed of a box section of perforated plywood or LVL boards (Fig. 3-b). This box section behaves at first as formwork for the reinforced concrete section, although at the same time it is also the support for the beams, so that the horizontal structure can be erected and concrete poured without having to wait for the supports to harden. The main function of the wooden elements is therefore to support the structure during the construction phase in which the concrete has yet to acquire the necessary strength.

Fig. 4 shows the construction process sequence. The TCC system developed clearly makes it possible to combine the use of reinforced concrete walls or cross-laminated timber (CLT) walls as complementary stabilising elements against horizontal forces. The system also makes it possible to easily include CLT facades and partitions. Fig. 5 shows computer-generated images of the completely erected system.

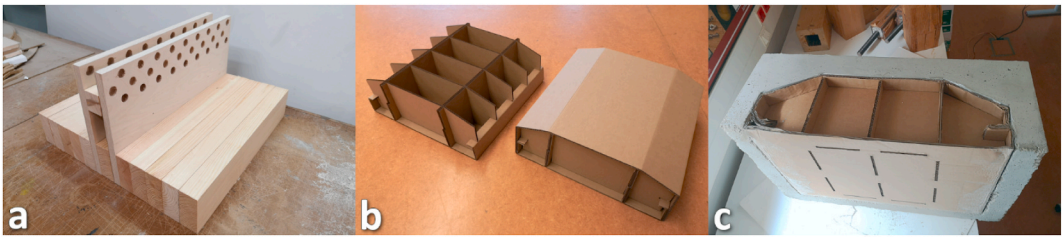

Fig. 2. a- Prototype of prefabricated flooring part. b- Light cardboard blocks during folding and erection. c- Integrity test of cardboard pieces during concrete pouring.

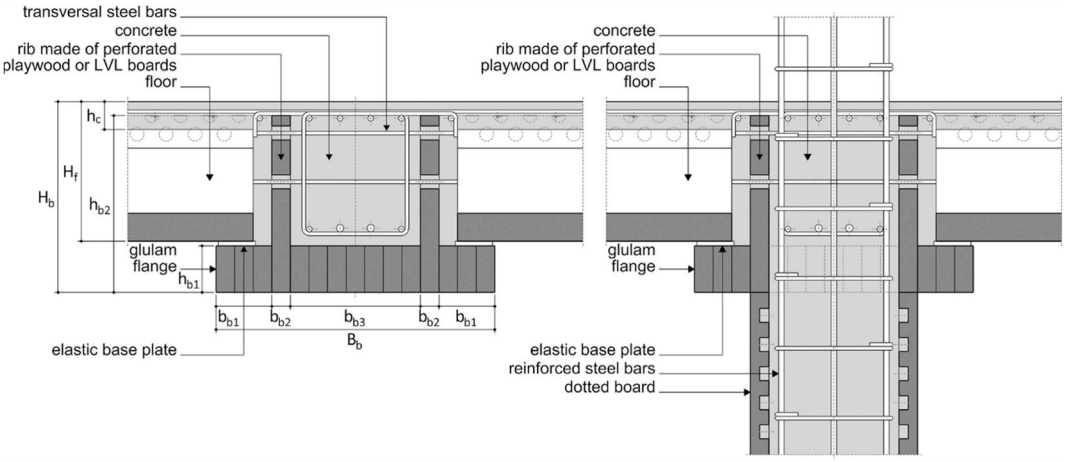

Fig. 3. a-Cross-section of the beam with flooring support. b-Beam-to-column connection.

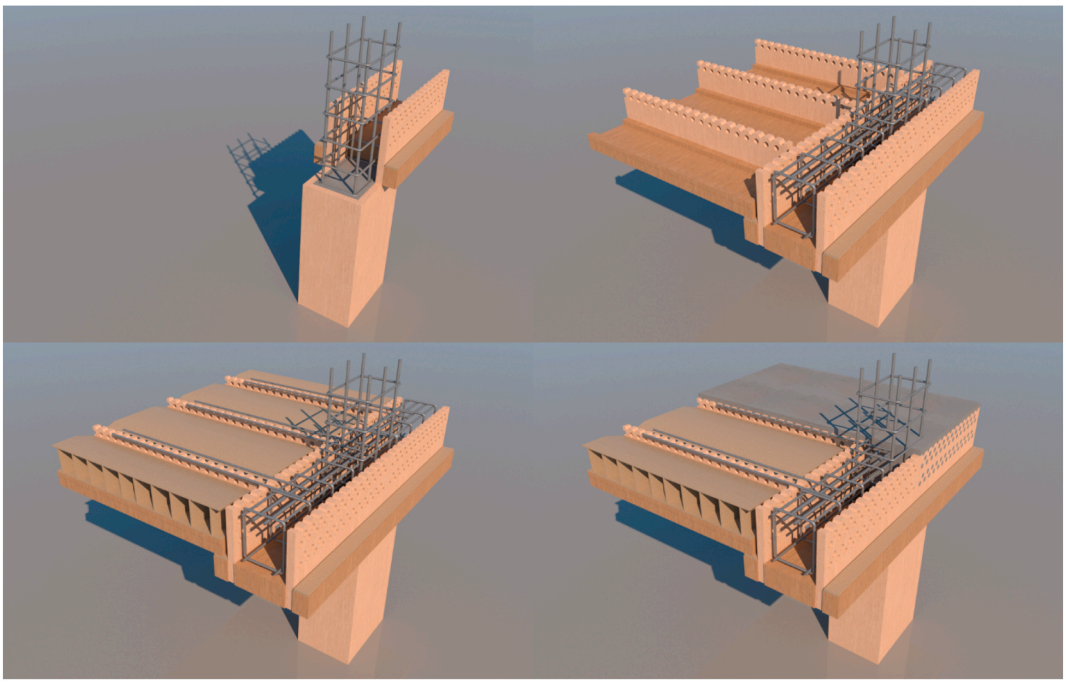

Fig. 4. Sequential erection process.

3. Test campaign

A test campaign was performed to validate the behaviour of the proposed system. Three types of tests were included which made it possible to obtain a preliminary evaluation of the fundamental elements which characterise the system: shear test of the timber-concrete connection, shear test along the glue line and delamination test of the glued planes.

3.1. Materials

The prototypes were made of the materials listed below:

- Birch plywood boards for the ribs of the pieces. Birch was selected to ensure a high strength against shear forces. The mechanical characteristics of the boards were supplied by the manufacturer, and they were as follows (Table 1):

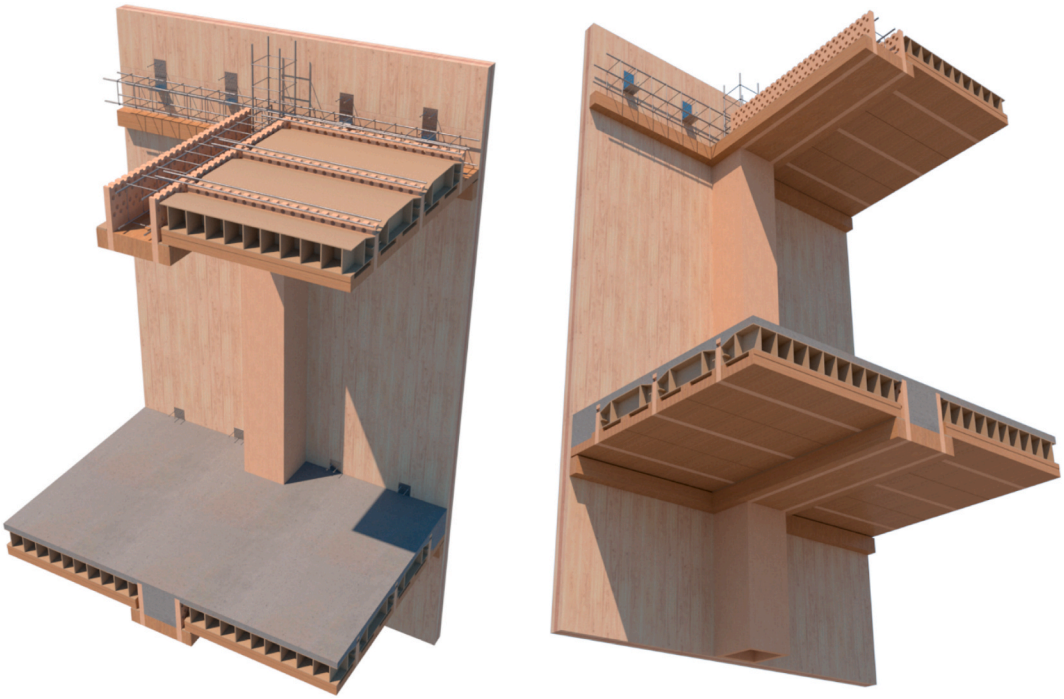

Fig. 5. Computer-generated images of the complete system combined with a CLT panel.

3.2. TIMBER-CONCRETE connection shear test

3.2.1. TEST specimens and setup

Twelve 480 × 300 × 300 mm test samples were prepared for the shear test, with the geometric characteristics shown in Fig. 6. A rib composed of two glued birch plywood boards was used, with two C24 strength class 40 mm thick pine wood strips between them. Two different board thickness was used to made the tests pieces: 15 mm and 21 mm. Three lines of 18 mm diameter staggered holes were drilled in the boards (the holes corresponding to each row are horizontally offset or displaced from their position in adjacent rows by a distance equal to half the horizontal spacing between holes). Concrete 50 mm–120 mm thick was poured onto the boards, which have a depth of 270 mm. The boards are 480 mm long and they were joined to the concrete slab along 450 mm, so that a gap was created which permitted slippage between the concrete and the boards during the shear test. 8 mm diameter B500S grade steel rebars were placed in each of the test pieces, three of them across the upper line of holes and two more arranged longitudinally.

The device shown in Fig. 7-a and b was designed for the shear test of the specimens, in which steel sections were used as support and reaction elements. The test pieces were supported on a 15 mm thick steel plate in a shape that reproduced the cross-section of the concrete, so that the boards were able to slip across the support under load. To prevent friction between the boards and the vertical section of the steel which balances the turning moment caused by the eccentric application of the load, a piece of Teflon® or PTFE was positioned between the reaction section and the specimen. Two loading procedures were used. In the first one, known as "Test T1", the load is applied through a steel distribution plate that occupies the whole length (270 mm) of the boards (Fig. 7-a). In the second procedure, named as "Test T2", the load is only applied over the part of the board which protrudes from under the concrete slab, i.e., 300–120 = 180 mm (Fig. 7-b). In this case, to guarantee the effectiveness of the device a cut was made in the boards at the depth where they connect with the concrete (Fig. 7-c).

The specimens were tested to failure using a push-out shear test according to EN 26891:1992 [39]. The specimens were firstly loaded up to 40% of the estimated failure load (F_{est}), keeping this load for 30 s. The load was then reduced to 10% of the estimated failure load, and this load was maintained for 30 s. The load was then finally increased until failure of the test piece or until slippage of 15 mm occurred. The load was applied at a constant speed of 0.2 times the estimated failure load (±25%) until 70% of the estimated failure load was reached. After this moment, the load was adjusted for displacement to achieve failure (due to failure or 15 mm slippage) in an additional test time of 3–5 min. Two transducers were fitted to record slippage in the intermediate phases established by the standard, one at each side of the test piece and halfway along its length, as is shown in Fig. 7-a y 7-b.

3.2.2. TEST results

Table 2 shows the results obtained. A high level of uniformity in the ultimate loads applied in each series can be observed. The way the load is applied visibly affects the result obtained. Applying the load on the smaller section (test T2) instead of along the whole rib (test T1) causes a 16.8% reduction in the average ultimate load value for the specimens made using two 15 mm boards, and of 11.3% for the specimens with 21 mm thick boards. This is logical, as the eccentricity in load application is increased when test T2 is used. Considering the average values of the ultimate load obtained using the most unfavourable method of load application (166.3 kN on 15

Table 1
Strength characteristics of the birch plywood boards, supplied by the manufacturer.

- C24 strength class pinewood, according to UNE 56544:2011 [34].
- Strength class GL28h GLT made of *Picea abies* [35] to form the flanges of the inverted T pieces.
- Upper concrete slab made with CEM II/A-M (V-L) 42.5 R cement, with a density of 346 kg/m^3. Sikafiber Force M − 48 polyolefin macrofibres were added (48 mm long, 465 MPa tensile strength, according to EN 14889–2:2008 [36] at a proportion of 4% in order to improve cracking behaviour caused by shrinkage). Compression characterisation tests were carried out according to UNE-EN 12390–3:2020 [37], obtaining an average strength at 28 days of 43.3 N/mm^2.
- 8 mm diameter B500S corrugated steel bars, according to UNE 36068:2011 [38] with a minimum elastic limit of the steel of $f_y \geq 500$ N/mm^2 and a failure load of $f_u \geq 550$ N/mm^2.

Timber, Nominal thickness [mm]	Number of plies	Charact. compression strength [N/mm^2]		Mean MOE in compression and tension [N/mm^2]		Charact. panel shear [N/mm^2]		Charact. planar shear [N/mm^2]		Mean MOR in panel shear [N/mm^2]		Mean MOR in planar shear [N/mm^2]	
		$f_{c,\parallel}$	$f_{c,\perp}$	$E_{t,c,\parallel}$	$E_{t,c,\perp}$	$f_{v,\parallel}$	$f_{v,\perp}$	$f_{r,\parallel}$	$f_{r,\perp}$	$G_{v,\parallel}$	$G_{v,\perp}$	$G_{r,\parallel}$	$G_{r,\perp}$
Birch 15	11	27.4	24.6	9223	8277	9.5		2.6	2.4	620		205	180
Birch 21	15	27.0	25.5	9093	8407	9.5		2.6	2.4	620		205	180

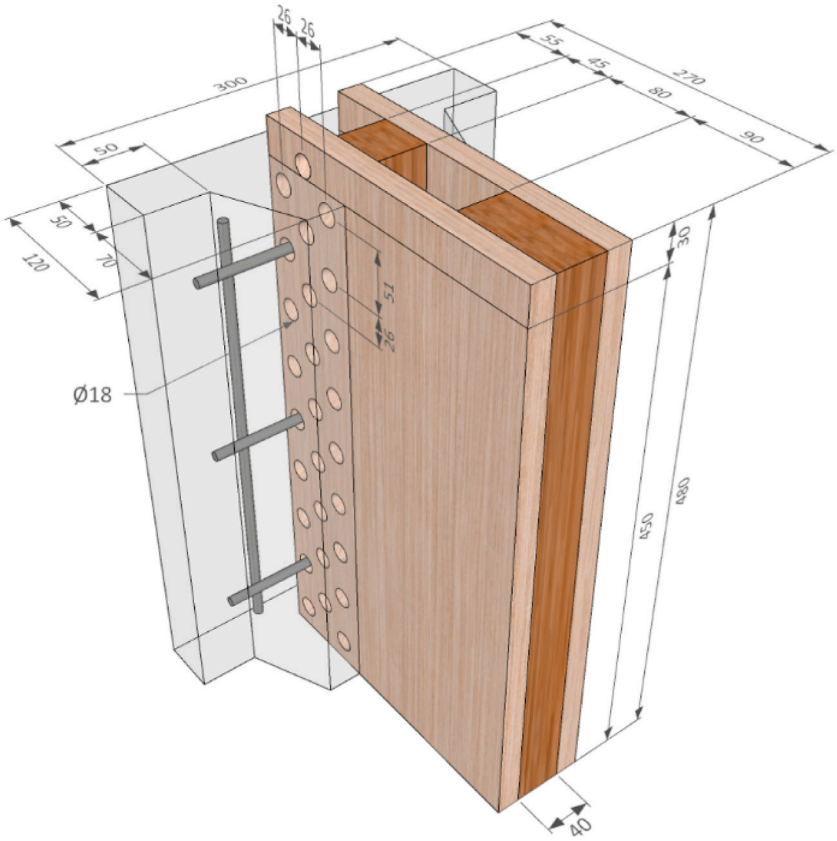

Fig. 6. Test specimens. Geometric characteristics.

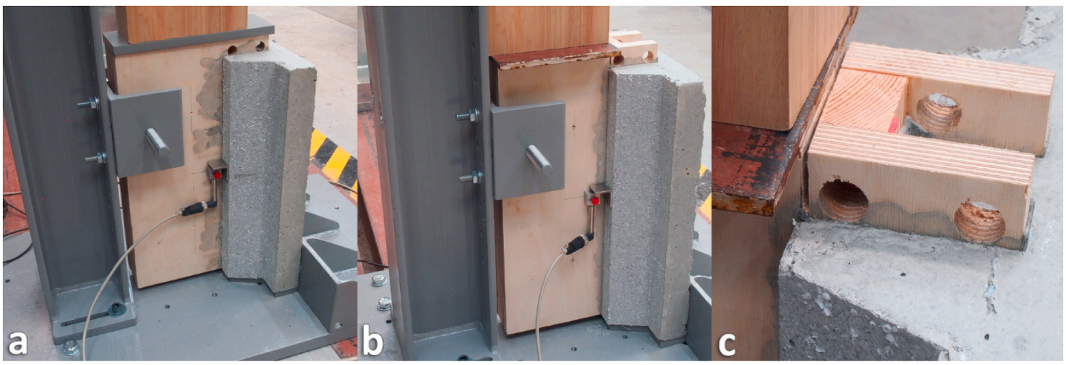

Fig. 7. a-Test T1. b-Test T2. c-Test T2 detail of the cut made in boards.

mm boards and 201.8 kN on 21 mm boards), the average shear stress, without discounting holes when calculating the resisting area, stands at 12.32 N/mm^2 and 10.68 N/mm^2 for the 15 mm and 21 mm boards, respectively. These values are very high, and they show the effective strength of the connection. On the other hand, the load-slip curves shown in Fig. 8 prove that these high strength values are attained with ductile behaviour that is present in all of the specimens tested.

Respecting the failure mode, it has to be pointed out that cracking of the concrete, basically in the area supporting the specimen in contact with the seating plate, was detected in several specimens (Fig. 9-a and 9-b). The cracks sloped down from the top edge of the boards. These cracks were detected after each of the specimens had been tested, and they had not cause failure of the joint. In all of the test pieces, regardless of the board thickness used and the loading system used, significant slippage of the boards respecting the section of concrete was detected (Fig. 9-c a 9-f) while the loading capacity of the joint remained. This indicates that this slippage derives from the combined effect of the crushing of the boards in the zone of the holes, generated by the concrete cylinders that pass through them, and the deformation of the steel rebar, thanks to the ductility shown by the joint in the load-slip graphs.

Table 2
Ultimate loads and stiffness modulus.

Type	Birch plywood	Test load method	Ultimate loads [kN]	Mean ultimate load [kN]	K04 [N/mm]	Mean K04 [N/mm]	Kser [N/mm]	Mean Kser [N/mm]
AB15C	2 × 15 mm	Test T1	201.1	199.8	179356	180478	172989	172475
			196.9		177971		177525	
			201.2		184107		166912	
AB15R	2 × 15 mm	Test T2	168.2	166.3	168857	161800	152781	150488
			163.8		172813		163360	
			166.9		143729		135324	
AB21C	2 × 21 mm	Test T1	231.9	227.6	171508	179470	164457	176558
			229.1		167383		170948	
			221.9		199519		194269	
AB21R	2 × 21 mm	Test T2	191.4	201.8	130697	140947	126014	139235
			202.6		141093		134642	
			211.5		151052		143827	

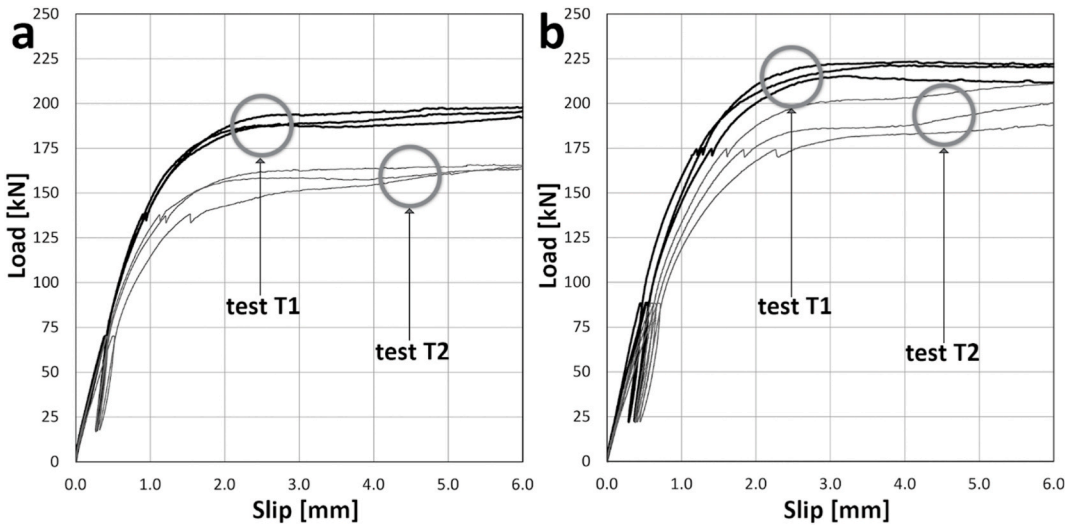

Fig. 8. Load-slip curves of the different types of specimen. a-Specimens with 15 mm board. b-Specimens with 21 mm board.

In terms of connection stiffness the results were also very homogeneous within each series of tests (Fig. 8). Moreover, the average values of K_{ser} obtained are 12.75% and 21.14% lower in the case of load application on the smaller section rather than on the complete section, for test pieces with 15 mm and 21 mm boards, respectively. In any case, the results indicate that the connection has a high degree of stiffness, as it offers high strength capacity with very low slippage values, the result of which is a high composite effect of the cross-section.

3.3. Shear test in the glue line

3.3.1. TEST specimens and setup

A prototype of the GLT flanges was made, and 12 test samples were extracted from this (Fig. 10-a). The specimens had dimensions of 390 × 50 × 50 mm. Each specimen consisted of 9 layers with 8 layers of glue (6 wood-wood and 2 wood-plywood). The test was performed according to the UNE-*EN* 14080:2013 standard [35] applying the load along the direction of the fibre (Fig. 10-b).

3.3.2. TEST results

The main aim of these tests was to verify the efficacy of the glued connection between the *Picea abies* wood and the birch plywood board, to provide information that would make it possible to specify the size of the needed contact surface between the lower layer of laminated wood and the central rib. The results obtained are shown in Table 3, and they prove the good behaviour of the connection in terms of strength as well as the efficacy of the glue, as in all cases failure occurred in the wood (Fig. 11).

3.4. Glue lines delamination test

3.4.1. TEST specimens and setup

A prototype of the flooring piece was made, and 8 test samples were extracted from this (Fig. 12). The specimens had dimensions of 195 × 75 × 77 mm. Each specimen consisted of 5 layers with 4 glue lines (3 wood-wood and 1 wood-plywood). The test was performed

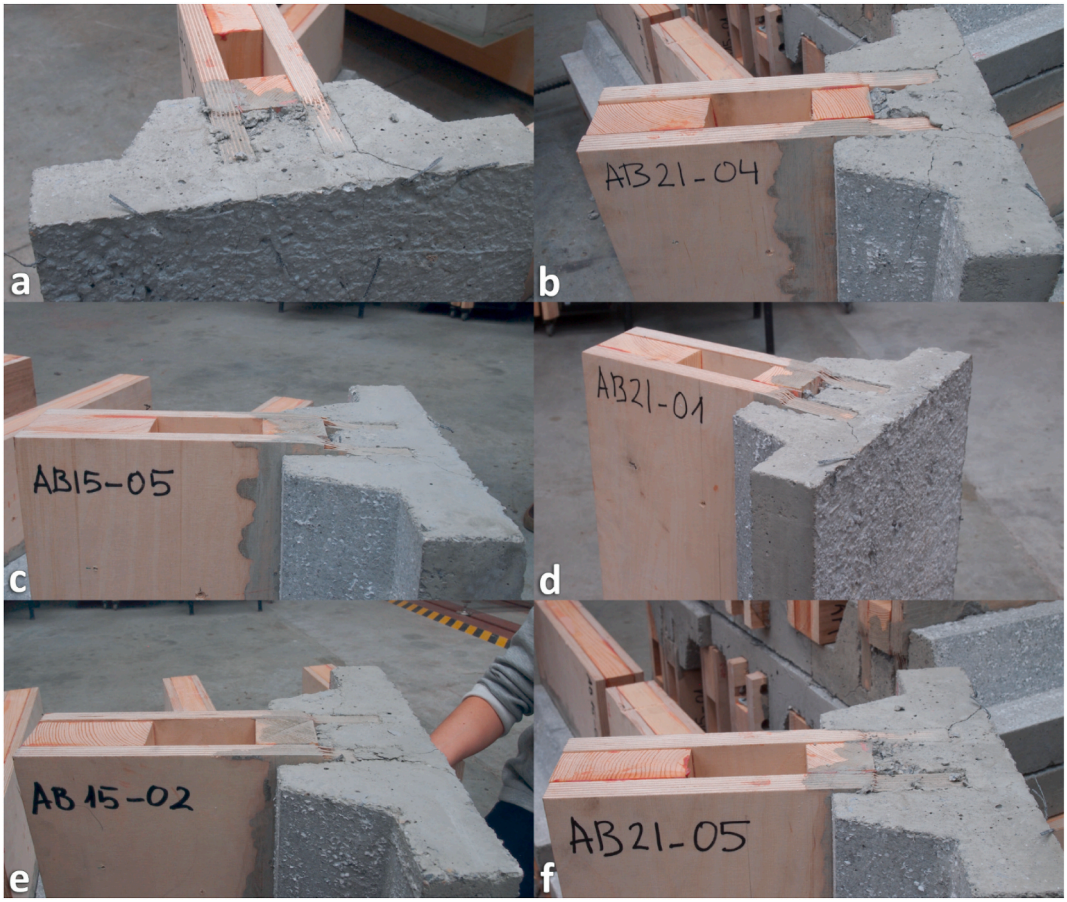

Fig. 9. a and b-Cracks in the concrete. c and d-Test T1, 15 and 21 mm boards. e and f-Test T2, 15 and 21 mm boards.

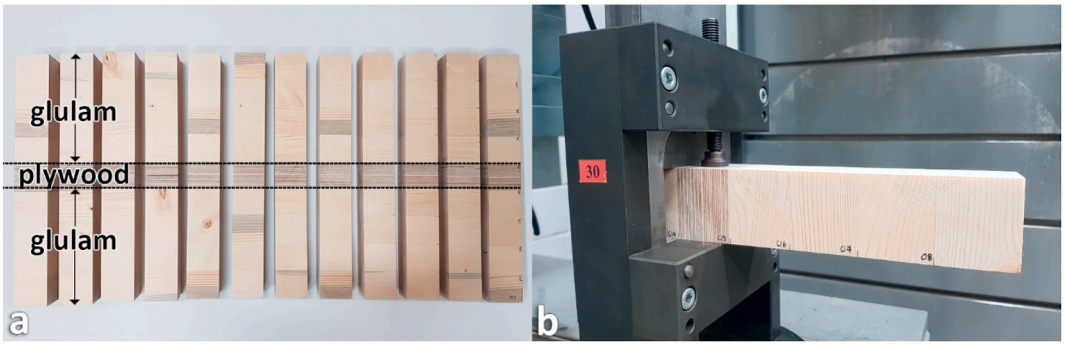

Fig. 10. Test specimens and shear test along the glue line.

Table 3
Results of the glue line shear test.

Glue line	Number of lines tested		Ultimate load F_u (kN)	Shear force resistance f_v (N/mm^2)	Failure of the wood (%)
Wood-wood	72	Average value	24	9.63	78
		Standard deviation	4	1.46	20
		C·V. (%)	15	15	25
Wood-plywood	24	Average value	18	7.16	100
		Standard deviation	3	0.99	1
		C·V. (%)	14	14	1

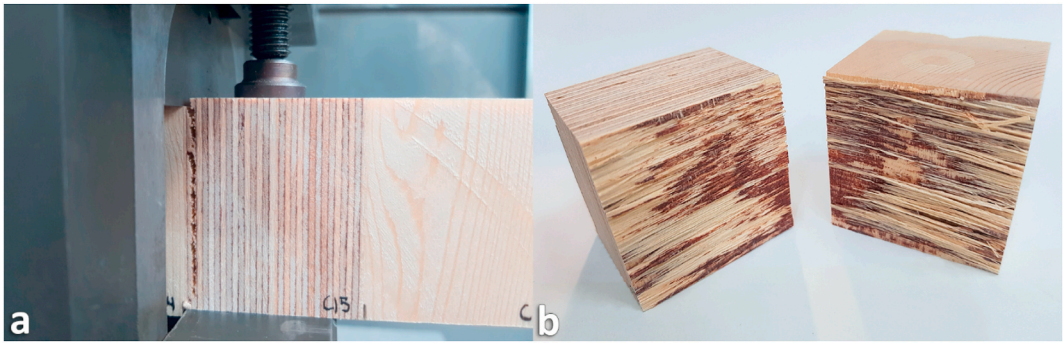

Fig. 11. a-Glue line shear test. b-Failure in the wood-plywood connection.

Fig. 12. Test pieces after the delamination tests.

according to the UNE-EN 14080:2013 standard [35], applying the B test cycle method, which consists of placing the weighted test pieces in an autoclave so that they are completely submerged. A vacuum of from 70 kPa to 85 kPa is created and maintained for 30 min. The vacuum is then eliminated and pressure from 500 kPa to 600 kPa is applied during 2 h. Finally, the test pieces are arranged in a drying chamber with at least 50 mm between them and with their heads parallel to the air current from 10 to 15 h at a temperature from 65 °C to 75 °C and relative humidity from 8% to 10%.

3.4.2. TEST results

No delamination of any type occurred in 19 of the 24 wood-wood glue lines; a maximum delamination occurred in the other 5 lines of 14%, 4%, 10%, 4% and 13%. In the case of the wood-plywood connection, in 5 of the 8 glue lines (Fig. 12) no type of delamination occurred, while in the other 3 the results were 6%, 9% and 4% delamination. Therefore, the results may be considered highly satisfactory, guaranteeing the integrity of the section glue lines.

4. System performance

The behaviour of the TCC component parts of the flooring system is quite complex because of the many factors that are involved: specific sizing of each element (flooring, beams and columns), span and distance between plans, boundary and loading conditions, stress-strain curves of the materials, creep of materials, amount of concrete reinforcement and cracking grade of concrete in tension and, in the case of timber, hygrothermal conditions. The model commonly used for the design process of TCC pieces is the Gamma method. It is a simplified method outlined in Eurocode 5–Annex B [40] and usually recommended [41,42]. The method allows to calculate an effective bending stiffness and to predict the internal actions based on reducing the axial stiffness of the compressed concrete slab as a function of the slip produced at the joint. Method assumptions consider the theory of linear elasticity in a beam under distributed load with a real span in the case of simply supported beam and an effective span equal to 0.8 of the relevant span for continuous beams. Girhammar [43] developed a simplified analysis method for composite beams with interlayer slip that can be applied to arbitrary boundary and loading conditions. This method has the advantage of giving results identical to those of the Gamma method for symmetrically simply supported beams while increasing its accuracy for other boundary conditions. Girhammar [43] has carried out an in-depth comparative analysis between its simplified method [43], the method recommended by Eurocode 5 [40] and the exact solution [44–46]; the results show that the error committed in the determination of the maximum deflection by the Gamma method is +0.4% in simply supported beams, −11.5% in pinned-clamped beams and up to −26.7% in the case of clamped-clamped beams. However, in the case of pinned-clamped and clamped-clamped beams, the percentage error can be substantially reduced if instead of considering an effective beam length equals 0.8 of the relevant length, values of 0.75 and 0.5774 of the relevant length

(distance between points of zero moment) are considered, respectively; in such a case, the error committed using the Gamma Method instead of the exact solution is reduced to −8,1% and −10,1%. In the case of the Girhammad Method this error is substantially lower (−4.1% y −1.0%). In any case, with the consideration made with respect to the effective beam length, the use of the Gamma method in boundary conditions other than that of simply supported pieces is applicable admitting an error in the estimation of deflections around 10%.

Floor preliminary sizing curves were prepared to show system performance, in order to know the possibilities offered by the system for its use in building structures, by establishing its capacities and adaptation to different situations of span, load and support conditions. Since no final sizing is intended, but simply to establish the appropriate range for the use of the system, the use of the Gamma method has been considered adequate based on its logical simplicity and its endorsed use in this field. In the analyses carried out, a conservative approach has been followed using the least favourable experimental result of K_{ser}, which corresponds to the test pieces composed of 21 mm boards and test T1. This K_{ser} value has been adopted to determine the bending stiffness for serviceability limit state assessments, reducing its value to 2/3 for ultimate limit state assessments.

Preliminary sizing curves show the span (L_f in Fig. 1-b) and the load for different load-bearing conditions and different depths (Fig. 13). The conditions considered to obtain these curves are described below.

The section of flooring shown in Fig. 1-c was considered. An upper concrete slab thickness of $h_c = 50$ mm and a GLT flange of $hf1 = 60$ mm were adopted. These values are considered to be the minimum possible, given building criteria and fire protection. Two $b_{f2} = 20$ mm thick plywood boards were considered for the rib. The weight of the floor under these conditions varies from a minimum of 1.68 kN/m^2, considering a total depth $H_f = 25$ cm and a width $B_f = 84$ cm, and a maximum of 1.81 kN/m^2 with $H_f = 35$ cm in combination with $B_f = 60$ cm. Two possible constructive solutions were considered on the above basis, both sufficiently representative

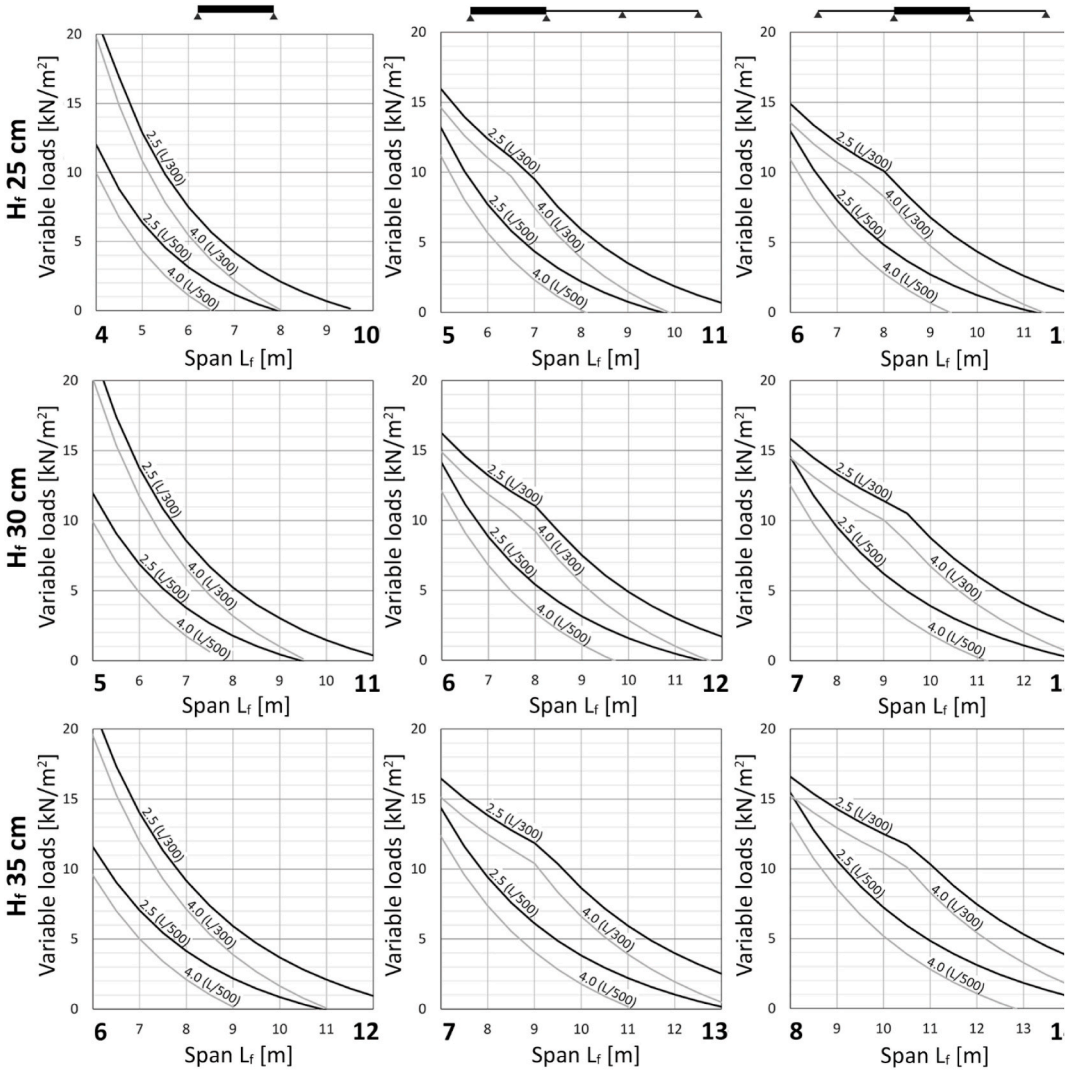

Fig. 13. Preliminary sizing curves for flooring. Permanent loads considered: G = 2.5 kN/m^2 (black) y Q = 4.0 kN/m^2 (grey). Deflection limits considered: L/300 and L/500.

of the possibilities present in building structures. The lightest considers a total permanent load value of 2.50 kN/m^2 (self-weight + constructive elements) and a total value of 4.00 kN/m^2 for the heaviest second case.

The characteristics of the materials considered are shown in Table 4.

A width of $B_f = 84$ cm was considered, with three different depths (25 cm, 30 cm and 35 cm), two deflection limitations (L/300 and L/500) and three support conditions: simply supported beam, extreme span in a continuous beam and internal span in a continuous beam. In the case of continuous floors, a conservative assumption in relation to bending moments distribution was used, considering equal moments at the supports and at the middle of span. The deflection limit was set considering the total deflection (instantaneous + creep). Creep deflection was calculated with the total permanent load and a 30% of the variable load.

The results obtained show that the shear force in the plywood-concrete connection ($F_{v,d}$) determines the limit load of the floor in short and highly loaded pieces. This situation is unusual in the type of buildings where it is planned to use this system. In the other situations, the load limit is conditioned by the serviceability limits when it is considered a simply support beam, or that of the continuous floor with a deflection limit of L/500. For the deflection limit of L/300 the load limit appears to be restricted by strength conditions in the low range of slenderness, after which it is also conditioned by the deflection.

Based on the design curves shown in Fig. 13, the slenderness ratios for a representative case of a residential building can be obtained (Table 5). A permanent load was considered of G = 3.25 k/m^2, which corresponds to a conventional constructive solution, an intermediate load between light (2.5 kN/m^2) and heavy (4.0 kN/m^2). A imposed load of Q = 2 kN/m^2 was adopted, corresponding to Category A of Eurocode 1 [47].

The above values give an idea of the extremely good performance of the system, which makes it possible to achieve high levels of slenderness. It is interesting to compare the proposed TCC system with all-concrete or all-wood solutions.

In concrete-only solutions, Eurocode 2 [48] sets specific span/depth ratios that make it possible to dispense with deformation calculations. In the case of slabs with geometrical quantities of the tension reinforcing in the centre of the span no greater than 0.5%, it sets span/depth ratios of 20, 26 and 30 for the conditions of simple supported pieces, extreme span and internal span with continuous pieces, respectively. However, two clarifications are necessary in connection with these coefficients. Firstly, the said ratios refer to the effective instead of the total depth of the piece. Considering a normal reinforcement cover of 30 mm, the final depth may be estimated in simplified form as 10% greater than the effective depth. This changes the above coefficients to 18.2 for simple supported beams and 23.6 and 27.3 for extreme and internal spans, respectively. The second point is that this table, when a span is greater than 7 m and partition walls are likely to suffer damage due to excessive deformations, must be affected by the 7/L ratio. This means that at above this range of spans, the coefficients would be even smaller. In any case, the span/depth ratios obtained for the TCC solution, in the most restrictive case which limits the total deflection to L/500, are significantly greater than those corresponding to reinforced concrete slabs (31.9% in pieces with two supports, 27.1% in extreme spans and 28.2% in internal spans). To elucidate the differences, a floor with a total depth of 25 cm with the TCC solution would have a self-weight of 1.80 kN/m^2 and would cover spans of 6.00 m, 7.50 m and 8.75 m for the three cases of support postulated. In order to achive these spans with a concrete solution, solid slab with a total thickness of 33 cm would be necessary, with a self-weight of 8.25 kN/m^2, i.e., 458% more, with all of the repercussions this would have for the increase in demands made on the beams, columns and foundations. If reinforced concrete ribs were used to reduce the weight, the self-weight could hardly fall below 3.00 kN/m^2, so that would represent an increase of 66.7% in comparison with the TCC solution. Finally, even if a floor of prestressed hollow-core concrete were used, in which case a 15 + 5 cm depth solution would be possible, the self-weight of the solution would amount to 3.90 kN/m^2, twice the weight of the TCC solution. To conclude, the TCC solution proposed here not only makes it possible to achieve slendernesses clearly superior to those obtained using reinforced concrete, as it also achieves this with significantly lower weights. This shows the efficacy of the solution, as well as its reduced material consumption.

In the case of wood-only solutions, we can certainly achieve degrees of slenderness that are similar to or even higher than is the case with box solutions. Additionally, these solutions are far lighter, at around 1/3 of the mixed solution proposed here. Nevertheless, this is only so for the case of simple supported solutions, as the difficulty of achieving rigid or semi-rigid joints means that continuous solutions are not usual, except those with solid pieces serving several spans, so that at average spans there is the additional problem of manufacturing and transporting long dimensions. Once we include continuity in comparative analysis, the advantages of the proposed solution are unquestionable. However, as well as continuity, the use of a thinner upper reinforced concrete slab (50 mm) gives the advantages of monolithism, with great stiffness in the plane for the transmission of horizontal forces and better behaviour in terms of acoustic, vibration and fire insulation. It even offers the possibility of using it for purposes such as a car park, with the upper slab as a finishing layer thanks to its surface durability and abrasion resistance.

To complete the evaluation of the overall system's performance, beam preliminary sizing curves were also prepared which relate the span L_b and the total load applied over a beam for different support conditions and different depths (Fig. 14). Gamma methodology was used taken into account the criteria set out at the beginning of this section.

The conditions used to obtain these curves are as follows:

The beam section shown in Fig. 3-a was considered. A thicker upper concrete slab was selected, at $h_c = 50$ mm and $h_{b1} = 100$ mm for the GLT flange. These dimensions are considered the minimum for constructive criteria and fire protection. Two ribs are used, each one of which is composed of a $b_{b2} = 40$ mm thick plywood board. Both ribs are $b_{b3} = 280$ mm apart for the concrete filling. This dimension was selected as it coincides with the minimum dimension considered in the supports. Likewise, the lower part of GLT protrudes laterally $b_{b1} = 120$ mm after the ribs to support the floor pieces. The material characteristics are the same as those described for the floors.

Frames with different spans and cross-section beam stiffness were analysed to determine bending moment distribution, to obtain cases that are representative of real situations. Three situations were considered which summarise and simplify the broad range of possibilities present in building structures. A single span beam between supports in which a negative bending moment of 43% of the

Table 4
Characteristics of the materials.

Concrete C25/30	$r = 2500$ kg/m^3	$f_{ck} = 25$ N/mm^2	$E_{cm} = 30.5$ kN/mm^2	$g_c = 1.50$	$f_{cd} = 16.67$ N/mm^2
GLT GL24h	$r = 430$ kg/m^3	$f_{m.k} = 24$ N/mm^2	$E_m = 11.0$ kN/mm^2	$g_m = 1.25$ $K_{mod} = 0.8$ $K_{def} = 0.6$	$f_{m,d} = 15.36$ N/mm^2
Birch plywood	$r = 700$ kg/m^3	$f_{m.k} = 37.2$ N/mm^2	$E_m = 9.3$ kN/mm^2	$g_m = 1.2$ $K_{mod} = 0.8$ $K_{def} = 0.6$	$f_{m,d} = 24.8$ N/mm^2 $F_{v,d} = 280$ kN/m ([a])

[a] This horizontal shear force value was selected according to the experimental results described in section 3.2.

Table 5
Slenderness ratios for the preliminary sizing for flooring in a residential building.

	Two supports		Extreme span		Internal span	
Deflection limits	$f \leq L/500$	$f \leq L/300$	$f \leq L/500$	$f \leq L/300$	$f \leq L/500$	$f \leq L/300$
Depth of floor H_f	$L_f/24$	$L_f/30$	$L_f/30$	$L_f/36$	$L_f/35$	$L_f/42$

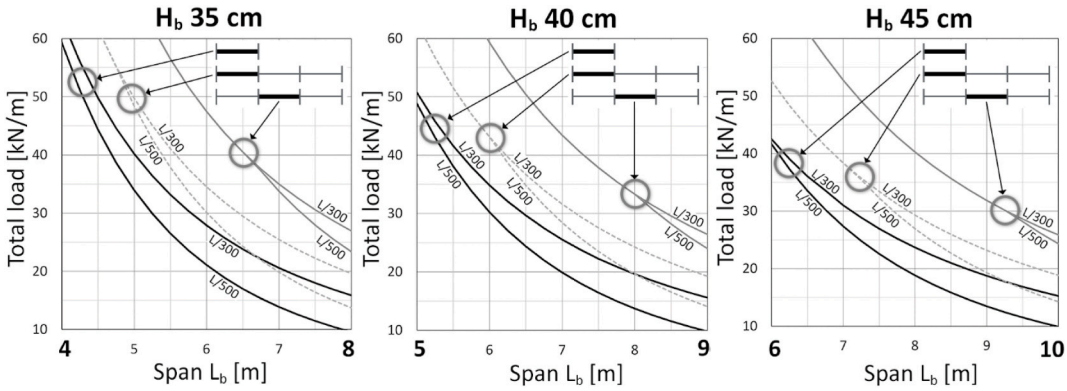

Fig. 14. Beam preliminary sizing curves. Limits of deflection considered: L/300 and L/500.

isostatic value has been assumed at both ends. An extreme beam in a continuous beam configuration with bending moments of 35% and 75% of the isostatic value for the extreme and internal joints, respectively. Finally, an internal beam in continuous beam configuration with negative bending moments of 66% of the isostatic value.

The load limit for span conditions depends on the ratio between permanent and variable loads within the total load. This is because these proportions influence the safety partial factors, in the ultimate limit state, as well as the amounts of creep deformation in the service limit state. Two representative extreme cases may be considered: on the one hand, a light constructive solution (with a permanent load of 2.50 kN/m^2) combined with a high public imposed load (5.00 kN/m^2 -Category C5 – Eurocode 1) [47]; in this case, the permanent load would represent 1/3 of the total applied load. Secondly, a heavy constructive solution (a permanent load of 4.00 kN/m^2) combined with a residential imposed load (2.00 kN/m^2 - Category A – Eurocode 1) [47]; in this case, the permanent load would represent 2/3 of the total applied load. When the results in both extreme situations are analysed, it may be seen that the differences between the loads at the ultimate limit state stand at around 3%, increasing these differences up to approximately 10% in the case of the service limit state. Given that these predimensioning curves are often designed to show the overall performance of a system, they have been simplified by adopting the minimum load corresponding to both situations.

The results are shown in Fig. 14. The value shown in the ordinate axis corresponds to the total lineal load on the beam, due to the action of permanent and variable loads.

The results indicate that for a single span beam, the load limit in the spans considered is the result of serviceability conditions. In both of the other cases (the extreme and internal continuous piece span), the load limit is conditioned in smaller spans by the ultimate limit state. It then goes on to be determined by the service limit $L_b/500$ at above a certain length of span, and this variable depends on the depth of the piece and whether it is an extreme or internal beam.

It is interesting to analyse the performance of the system as a whole, beams and floors, considering a representative case of loads in a residential building. Adopting $G = 3.25$ k/m^2 (including self-weight) and $Q = 2$ kN/m^2, assuming a structure formed of frames and continuous floors with a strict deflection limit for both elements of L/500, to prevent damage to partition walls and constructive elements, the following results are obtained. With a floor depth $H_f = 25$ cm it would be possible to achieve spans of 7.50 m, giving rise to a linear load on the beam of 39.4 kN/m. With a beam depth of $H_b = 35$ cm the achievable span under this load would be 5.3 m, in the case of the extreme span, and 6.5 m for the internal span. Increasing the depth of the beam to 40 cm, the achievable spans would then

be 6.1 m and 7.4 m in extreme and internal spans, respectively. Considering an average value of spans between extreme and internal spans, the proposed system would make it possible to achieve spans without columns of 45 m^2–50 m^2 with floors 25 cm depth and beams 35 cm, in the first case, and beams 40 cm depth in the second case. The above surface areas would increase to 55 m^2 and 60 m^2 if the limitation on deflection under total load were reduced to L/300 instead of L/500. These solutions would be possible with a structural self-weight of only 1.80 kN/m^2 (2.10 kN/m^2 to 2.20 kN/m^2 including the self-weight of the beams).

As well as the advantages in terms of the performance of the proposed TCC system, two other aspects of the constructive system stand out. The first of these is that fewer auxiliary resources are needed for execution, thanks to the lower self-weight of the constitutive elements. The timber pieces in an inverted T cross-section weigh from a minimum of 0.32 kN/m^2 for a width of 84 cm and a total depth of 25 cm, up to 0.39 kN/m^2 for a width of 60 cm and a total depth of 35 cm. This means that when considering the least favourable situation of 0.39 kN/m^2, the weight of each piece used to create a 10 m span floor is 4.68 kN for inverted π cross-section of 1.20 m. Even if 2.40 m wide pieces are used, the total weight is under 10 kN, and this makes it possible to use normal on-site cranes, contrary to what occurs with other types of prefabricated parts such as prestressed concrete hollow-core slabs.

The other question refers to the partially self-supporting nature of the system. The parts which form the floor as well as the beams only require a single line of formwork props arranged in the centre of the span. This makes it possible to use a small number of props and speeds up construction. The central support of the panels prior to the concrete being poured also makes it easily possible to apply a precamber to the pieces, as the discontinuity between the two sections of the boards which form the ribs of the T-shaped piece (Fig. 1-b) causes a reduction in stiffness at this point. This facilitates the creation of a camber in the pieces by simply making the central formwork prop slightly higher than the end supports of the beams. This precamber allows to counterbalance the deformations due to permanent loads and those generated by the shrinkage of the concrete poured in situ.

Thus definitively, use of the proposed TCC system makes it possible to take advantages of both materials, achieving semi-rigid connections between elements and slender solutions that combine strength with a high degree of lightness. These characteristics are accompanied by ease and speed of installation, as well as favourable behaviour in other building properties, such as fire resistance and thermal and acoustic insulation.

5. Conclusions

This complete solution for the execution of building structures uses mixed timber-concrete sections that make efficient use of the mechanical qualities of both materials.

The system is composed of floors and beams based on timber prefabricated pieces, which are formed by a GLT flange glued to one or more plywood or LVL ribs that are anchored to an upper concrete slab that is poured in situ. The pieces may be prefabricated in a T-shape (with a single rib), in π - shape (two ribs), or with multiple ribs in wider pieces to reduce assembly operations.

The basis of the system consists of the timber-concrete connection by means of drilling holes in the ribs through which the concrete poured in situ penetrates. The connection is complemented by the arrangement of reinforcing bars through the perforations in the board to improve the ductility of the connection.

Three test campaigns were performed to validate the design of the proposed cross-section:

- Shear testing of the timber-concrete connection using test pieces with a timber-concrete connection length of 450 mm. The results were very homogeneous in terms of the ultimate load and slip modulus, while the joint also displayed ductile behaviour. In the least favourable test device, average ultimate load values were obtained of 166.3 kN for the case with two 15 mm thick birch wood boards and 201.8 kN with two 21 mm thick boards. The average values of K_{ser} in both cases were 150488 N/mm and 139235 N/mm, respectively, which indicate a high degree of stiffness while taking great advantage of the composite effect.
- Shear testing along the wood-wood and wood-plywood glue line, obtaining average values of 9.63 N/mm^2 (wood-wood) and 7.16 N/mm^2 (wood-plywood). Failure did not occur in any of the test pieces along the glue line.
- Delamination testing of the glued planes (wood-wood and wood-plywood), with satisfactory results that guarantee the integrity of the section as designed, under demanding hygrothermal conditions.

The Gamma method was used to prepare preliminary sizing curves for the floors and beams, to show system performance. In a residential building with permanent loads of G = 3.25 kN/m^2, usage imposed load of Q = 2.0 kN/m^2 and a deflection limit of L/500 the floor attained slenderness ratios of L_f/24, L_f/30 and L_f/35 in cases involving isolated, extreme and internal spans, respectively, and a floor self-weight of 1.80 kN/m^2. These degrees of slenderness are clearly higher than can be achieved with solid or ribbed reinforced concrete slabs (L_f/18,2 in isolated spans, L_f/23.6 and L_f/27.3 in extreme and internal spans, respectively). This increased slenderness is also achieved with an extremely important self-weight reduction in comparison with concrete-only solutions, which makes it possible to reduce the need for auxiliary facilities during construction.

In comparison with wood-only solutions, the advantages of the system consist of its easy-to-make continuous and semi-rigid joints, offering monolithism, great planar stiffness for the transmission of horizontal forces, and better behaviour against vibration and fire.

Author statement

The revision and changes have been approved by all the authors.

Declaration of competing interest

The authors declare that they have no known competing financial interests or personal relationships that could have appeared to

influence the work reported in this paper.

Acknowledgments

This study is part of the research project "High-performance timber-concrete-composite hollow-core floors for sustainable and eco-efficient construction (AlveoTCC)". The study developed was financed by the Spanish Ministry of Science and Innovation.

References

[1] United Nations Environment Programme, Global status report for buildings and construction. Towards a zero-emissions, efficient and resilient buildings and construction sector, Nairobi (2021).
[2] J. Li, B. Rismanchi, T. Ngo, Feasibility study to estimate the environmental benefits of utilising timber to construct high-rise buildings in Australia, Build. Environ. 147 (January 2019), https://doi.org/10.1016/j.buildenv.2018.09.052, 108–120.
[3] O.A.B. Hassan, F. Öberg, E. Gezelius, Cross-laminated timber flooring and concrete slab flooring: a comparative study of structural design, economic and environmental consequences, J. Build. Eng. 26 (November 2019), 100881.
[4] I. Lukić, M. Premrov, A. Passer, V. Žegarac Leskovar, Embodied energy and GHG emissions of residential multi-storey timber buildings by height – a case with structural connectors and mechanical fasteners, Energy Build. 252 (1) (December 2021), 111387, https://doi.org/10.1016/j.enbuild.2021.111387.
[5] A. Ahmad, Q.-J. Liu, S. Nizami, A. Mannan, S. Saeed, Carbon emission from deforestation, forest degradation and wood harvest in the temperate region of Hindukush Himalaya, Pakistan between 1994 and 2016, Land Use Pol. 78 (2018) 781–790.
[6] M. Knauf, Market potentials for timber-concrete composites in Germany's building construction sector, Eur.. J. Wood Wood Prod. https://doi.org/10.1007/s00107-016-1136-9, 2017, 75,639-649.
[7] A. Dias, J. Skinner, K. Crews, T. Tannert, Timber-concrete-composites increasing the use of timber in construction, Eur.. J. Wood Wood Prod 74 (2016) 443–451, https://doi.org/10.1007/s00107-015-0975-0.
[8] D. Yeoh, M. Fragiacomo, M. De Franceschi, K. Heng Boon, State of the art on timber-concrete composite structures: literature review, J. Struct. Eng. 137 (2011) 1085–1095, https://doi.org/10.1061/(ASCE)ST.1943-541X.0000353.
[9] S. Di Nino, A. Gregori, M. Fragiacomo, Experimental and numerical investigations on timber-concrete connections with inclined screws, Eng. Struct. 209 (2020), 109993, https://doi.org/10.1016/j.engstruct.2019.109993.
[10] H. Du, X. Hu, Z. Sun, Y. Meng, G. Han, Load carrying capacity of inclined crossing screws in glulam-concrete composite beam with an interlayer, Compos. Struct. 245 (2020), 112333, https://doi.org/10.1016/j.compstruct.2020.112333.
[11] Y. Zhang, G.M. Raftery, P. Quenneville, Experimental and analytical investigations of a timber-concrete composite beam using a hardwood interface layer, J. Struct. Eng. 145 (2019), 04019052, https://doi.org/10.1061/(ASCE)ST.1943-541X.0002336.
[12] M.A.H. Mirdad, Y.H. Chui, Load-slip performance of Mass Timber Panel-Concrete (MTPC) composite connection with self-tapping screws and insulation layer, Construct. Build. Mater. 213 (2019) 696–708, https://doi.org/10.1016/j.conbuildmat.2019.04.117.
[13] H. Du, X. Hu, Z. Xie, H. Wang, Study on shear behavior of inclined cross lag screws for glulam-concrete composite beams, Construct. Build. Mater. 224 (2019) 132–143, https://doi.org/10.1016/j.conbuildmat.2019.07.035.
[14] W.M. Sebastian, M. Piazza, T. Harvey, T. Webster, Forward and Reverse shear transfer in beech LVL-concrete composites with singly inclined coach screw connectors, Eng. Struct. 175 (2018) 231–244, https://doi.org/10.1016/j.engstruct.2018.06.070.
[15] K.Q. Mai, A. Park, K. Lee, Experimental and numerical performance of shear connections in CLT–concrete composite floor, Mater. Struct. 51 (2018) 84, https://doi.org/10.1617/s11527-018-1202-3.
[16] L. Marchi, R. Scotta, L. Pozza, Experimental and theoretical evaluation of TCC connections with inclined self-tapping screws, Mater. Struct. 50 (2017) 180, https://doi.org/10.1617/s11527-017-1047-1.
[17] W.M. Sebastian, J. Mudie, G. Cox, M. Piazza, R. Tomasi, I. Giongo, Insight into mechanics of externally indeterminate hardtimber-concrete composite beams, Construct. Build. Mater. 102 (2016) 1029–1048, https://doi.org/10.1016/j.conbuildmat.2015.10.015.
[18] C. Martins, A.M.P.G. Dias, R. Costa, P. Santos, Environmentally friendly high performance timber–concrete panel, Construct. Build. Mater. 102 (2016) 1060–1069, https://doi.org/10.1016/j.conbuildmat.2015.07.194.
[19] M. Fragiacomo, E. Lukaszewska, Time-dependent behavior of timber–concrete composite floors with prefabricated concrete slabs, Eng. Struct. 52 (2013) 687–696, https://doi.org/10.1016/j.engstruct.2013.03.031.
[20] N. Khorsandnia, H. Valipour, M. Bradford, Deconstructable timber-concrete composite beams with panelised slabs: finite element analysis, Construct. Build. Mater. 163 (2018) 798–811, https://doi.org/10.1016/j.conbuildmat.2017.12.169.
[21] M. Fragiacomo, C. Amadio, L. MacOrini, Short- and long-term performance of the "Tecnaria'' stud connector for timber-concrete composite beams, Mater. Struct. 40 (2007) 1013–1026, https://doi.org/10.1617/s11527-006-9200-2.
[22] B. Shan, Y. Xiao, W.L. Zhang, B. Liu, Mechanical behavior of connections for glubam-concrete composite beams, Construct. Build. Mater. 143 (2017) 158–168, https://doi.org/10.1016/j.conbuildmat.2017.03.136.
[23] E. Lukaszewska, H. Johnsson, M. Fragiacomo, Performance of connections for prefabricated timber–concrete composite floors, Mater. Struct. 41 (2008) 1533–1550, https://doi.org/10.1617/s11527-007-9346-6.
[24] E. Martín, J. Estévez, D. Otero, F. Suárez, Discontinuous π-form steel shear connectors in timber-concrete composites. An experimental approach, Eng. Struct. 216 (2020), 110719, https://doi.org/10.1016/j.engstruct.2020.110719.
[25] F. Suárez, J. Estévez, E. Martín, D. Otero, Perforated shear + reinforcement bar connectors in a timber-concrete composite solution, Analytical and numerical approach, Composites Part B: Engineering 156 (2019) 138–147. https://doi.org/10.1016/j.compositesb.2018.08.074.
[26] W.M. Sebastian, Switch from connection ductility to reinforcement ductility with curvature reversal in timber-concrete composites, Construct. Build. Mater. 229 (2019), 116886, https://doi.org/10.1016/j.conbuildmat.2019.116886.
[27] N. Naud, L. Sorellia, A. Salenikovich, S. Cuerrier-Auclair, Fostering GLULAM-UHPFRC composite structures for multi-storey buildings, Eng. Struct. 188 (2019) 406–417, https://doi.org/10.1016/j.engstruct.2019.02.049.
[28] J. Mudie, W.M. Sebastian, J. Norman, I.P. Bond, Experimental study of moment sharing in multi-joist timber-concrete composite floors from zero load up to failure, Construct. Build. Mater. 225 (2019) 956–971, https://doi.org/10.1016/j.conbuildmat.2019.07.137.
[29] J. Kanócz, V. Bajzecerová, Š. Steller, Timber–Concrete composite elements with various composite connections Part 2: grooved connection, Wood Res. 59 (2014) 627–638.
[30] H. Du, X. Hu, G. Han, D. Shi, Experimental and analytical investigation on flexural behaviour of glulam-concrete composite beams with interlayer, J. Build. Eng. 38 (2021), 102193, https://doi.org/10.1016/j.jobe.2021.102193.
[31] A.M.P.G. Dias, U. Kuhlmann, K. Kudla, S. Mönch, A.M.A. Dias, Performance of dowel-type fasteners and notches for hybrid timber structures, Eng. Struct. 171 (2018) 40–46, https://doi.org/10.1016/j.engstruct.2018.05.057.
[32] L. Boccadoro, S. Zweidler, R. Steiger, A. Frangi, Bending tests on timber-concrete composite members made of beech laminated veneer lumber with notched connection, Eng. Struct. 132 (2017) 14–28, https://doi.org/10.1016/j.engstruct.2016.11.029.
[33] D. Yeoh, M. Fragiacomo, M. De Franceschi, A.H. Buchanan, Experimental tests of notched and plate connectors for LVL-concrete composite beams, J. Struct. Eng. 137 (2011) 261–269, https://doi.org/10.1061/ASCEST.1943-541X.0000288.
[34] UNE 56544, Visual grading for structural sawn timber, Coniferous timber (2011).
[35] EN 14080, Timber structures. Glued laminated timber and glued solid timber. Requirements, European Committee for Standardization, Brussels, 2013, 2013.

[36] EN 14889–2, Fibres for Concrete - Part 2: Polymer Fibres. Definitions, Specifications and Conformity, European Committee for Standardization, Brussels, 2008, 2008.
[37] EN 12390–12393, Testing hardened concrete. Part 3: compressive strength of test specimens. General principles for the determination of strength and deformation characteristics, Brussels. European Committee for Standardization 2009 (2009).
[38] UNE 36068, Ribbed Bars of Weldable Steel for the Reinforcement of Concrete, Aenor, Madrid, 2011, 2011.
[39] EN 26891, Timber structures. Joints made with mechanical fasteners. General principles for the determination of strength and deformation characteristics. (ISO 6891:1983), Brussels. European Committee for Standardization (1992).
[40] EN 1995-1-1, Eurocode 5. Design of timber structures, Brussels. European Committee for Standardization (2016).
[41] A. Dias, J. Schänzlin, P. Dietsch (Eds.), Design of Timber-Concrete Composite Structures: A State-Of-The-Art Report by COST Action FP1402/WG 4, Shaker Verlag Aachen, 2018.
[42] N. Khorsandnia, H.R. Valipour, K. Crews, Structural response of timber-concrete composite beams predicted by finite element models and manual calculations, in: 2013 World Congress on Advances in Structural Engineering and Mechanics (ASEM13). Korea, 2013.
[43] U.A. Grihammar, A simplified analysis method for composite beams with interlayer slip, Int. J. Mech. Sci. 51 (2009) 515–530.
[44] U.A. Girhammar, V.K.A. Gopu, Analysisof P–D effect in composite concrete-timber beam-columns, Proceedings of the Institution of Civil Engineers—Research and Theory (1991) 39–54.
[45] U.A. Girhammar, V.K.A. Gopu, Composite beam-columns withinter layer slip—exact analysis, ASCE Journal of Structural Engineering 119 (4) (1993) 1265–1282.
[46] U.A. Girhammar, D. Pan, Exact static analysis of partially composite beams and beam-columns, Int. J. Mech. Sci. 49 (2007) 239–255.
[47] EN 1991-1-1, Eurocode 1. Actions on structures, Brussels. European Committee for Standardization (2019).
[48] EN 1995-1-1, Eurocode 2. Design of concrete structures, Brussels. European Committee for Standardization (2016).